

# Implications of the CMS search for $W_R$ on grand unification

Triparno Bandyopadhyay,<sup>a</sup> Biswajoy Brahmachari<sup>b</sup> and Amitava Raychaudhuri<sup>a</sup>

<sup>a</sup>*Department of Physics, University of Calcutta,  
92 Acharya Prafulla Chandra Road, Kolkata 700009, India*

<sup>b</sup>*Department of Physics, Vidyasagar Evening College,  
39 Sankar Ghosh Lane, Kolkata 700006, India*

*E-mail:* [gondogolegogol@gmail.com](mailto:gondogolegogol@gmail.com), [biswa.brahmac@gmail.com](mailto:biswa.brahmac@gmail.com),  
[palitprof@gmail.com](mailto:palitprof@gmail.com)

**ABSTRACT:** The CMS experiment at the Large Hadron Collider has reported a  $2.8\sigma$  excess in the  $(2e)(2jets)$  channel around 2.1 TeV. Interpretation of this data is reconsidered in terms of the production of a right-handed weak gauge boson,  $W_R$ , of the left-right symmetric model and in an SO(10) grand unified theory abiding by the Extended Survival Hypothesis. The left-right symmetric model can be consistent with this excess if (a) the heavy right-handed neutrino has a mass near  $W_R$ , or (b) if  $g_L \neq g_R$ , or (c) the right-handed CKM matrix is nontrivial. Combinations of the above possibilities are also viable. A  $W_R$  with a mass in the TeV region if embedded in SO(10) is not compatible with  $g_L = g_R$ . Rather, it implies  $0.64 \leq g_R/g_L \leq 0.78$ . Further, a unique symmetry-breaking route — the order being left-right discrete symmetry breaking first, followed by  $SU(4)_C$  and finally  $SU(2)_R$  — to the standard model is picked out. The  $L \leftrightarrow R$  discrete symmetry has to be broken at around  $10^{16}$  GeV. The grand unification scale is pushed to  $10^{18}$  GeV making the detection of proton decay in ongoing searches rather unlikely. The  $SU(4)_C$  breaking scale can be at its allowed lower limit of  $10^6$  GeV so that  $n - \bar{n}$  oscillation or flavour changing processes such as  $K_L \rightarrow \mu e$  and  $B_{d,s} \rightarrow \mu e$  may be detectable. The Higgs scalar multiplets responsible for SO(10) symmetry breaking at various stages are uniquely identified so long as one adheres to a minimalist principle. We also remark, *en passant*, about a partially unified Pati-Salam model.

**KEYWORDS:** GUT, Beyond Standard Model

**ARXIV EPRINT:** [1509.03232](https://arxiv.org/abs/1509.03232)

---

## Contents

<b>1</b>	<b>Introduction</b>	<b>1</b>
<b>2</b>	<b>CMS <math>W_R</math> search result and the left-right symmetric model</b>	<b>3</b>
2.1	A $W_R$ signal?	4
<b>3</b>	<b>SO(10) grand unification</b>	<b>6</b>
3.1	Symmetry breaking	6
3.2	Scalar structure and the Extended Survival Hypothesis (ESH)	7
3.3	Renormalisation group equations	9
<b>4</b>	<b>Low energy expectations from unification</b>	<b>10</b>
4.1	Pati-Salam partial unification	10
4.2	Left-right symmetry and unification	11
<b>5</b>	<b>The three routes of SO(10) symmetry breaking</b>	<b>12</b>
5.1	The DRC route	12
5.2	The CDR route	12
5.3	The DCR route	14
<b>6</b>	<b>SO(10) unification with <math>M_R \sim \mathcal{O}(\text{TeV})</math></b>	<b>16</b>
6.1	Pati-Salam partial unification for the maximum-step case	16
6.2	Coupling unification for the maximum-step case	16
6.3	The $M_D = M_U$ case	17
6.4	Two-loop comparison	18
6.5	Additional scalars: two examples	19
<b>7</b>	<b>Summary and conclusions</b>	<b>20</b>

---

## 1 Introduction

The discovery of the Higgs boson at the Large Hadron Collider (LHC) at CERN is a major milestone of the successes of the standard model (SM) of particle physics. Indeed, with all the quarks and leptons and force carriers of the SM now detected and the source of spontaneous symmetry breaking identified there is a well-deserved sense of satisfaction. Nonetheless, there is a widely shared expectation that there is new physics which may be around the corner and within striking range of the LHC. The shortcomings of the standard model are well-known. There is no candidate for dark matter in the SM. The neutrino is massless in the model but experiments indicate otherwise. At the same time the utter

smallness of this mass is itself a mystery. Neither is there any explanation of the matter-antimatter asymmetry seen in the Universe. Besides, the lightness of the Higgs boson remains an enigma if there is no physics between the electroweak and Planck scales.

Of the several alternatives of beyond the standard model extensions, the one on which we focus in this work is the left-right symmetric (LRS) model [1–5] and its embedding within a grand unified theory (GUT). Here parity is a symmetry of the theory which is spontaneously broken resulting in the observed left-handed weak interactions. The left-right symmetric model is based on the gauge group  $SU(2)_L \times SU(2)_R \times U(1)_{B-L}$  and has a natural embedding in the  $SU(4)_C \times SU(2)_L \times SU(2)_R$  Pati-Salam model [2] which unifies quarks and leptons in an  $SU(4)_C$  symmetry. The Pati-Salam symmetry is a subgroup of  $SO(10)$  [6, 7]. These extensions of the standard model provide avenues for the amelioration of several of its shortcomings alluded to earlier.

The tell-tale signature of the LRS model would be observation of the  $W_R$ . At the LHC the CMS collaboration has searched for the on-shell production of a right-handed charged gauge boson [8] using the process:<sup>1</sup>

$$pp \rightarrow W_R \rightarrow 2j + ll. \tag{1.1}$$

In the above  $l$  stands for a charged lepton, and  $j$  represents a hadronic jet.

The CMS collaboration has examined the implication of its findings in the context of a left-right symmetric model where the left and right gauge couplings are equal ( $g_L = g_R$ ) and also the  $W_R$  coupling to a charged lepton,  $l$ , and its associated right-handed neutrino,  $N_l$ , is diagonal with no leptonic mixing,<sup>2</sup> (i.e.,  $V_{N_l l} = 1$ ). In the  $l = e$  channel the data shows a  $2.8\sigma$  excess near 2.1 TeV. Also, regions in the  $M_{N_l} - M_{W_R}$  plane disfavoured by the data, within an LRS theory with  $g_L = g_R$ , have been exhibited. After production, the  $W_R$  decays through  $W_R \rightarrow lN_l$  in the first stage. An associated signal of this process will be a peak at  $M_{N_l}$  in one of the  $lj\bar{j}$  invariant mass combinations. CMS has not observed the latter. One possibility may be that the produced  $N_l$  has a substantial coupling to the  $\tau$ -lepton [13, 14] —  $V_{N_l \tau}$  is not small. Here we keep  $M_{N_l}$  as a parameter of the model.

Within the LRS model there is room to admit the possibility of  $g_L \neq g_R$ . Interpretation of the CMS result in the presence of such a coupling asymmetry has also been taken up [15–17] keeping  $M_{N_l} = M_{W_R}/2$  and the implications for grand unification and baryogenesis explored. In [15, 16] the coupling parameter  $V_{N_l l}$  is also allowed to deviate from unity. Other interpretations of the excess have also appeared, for example, in [13–20].

In a left-right symmetric model emerging from a grand unified theory, such as  $SO(10)$ , one has a discrete symmetry  $SU(2)_L \leftrightarrow SU(2)_R$  — referred to as D-parity [21, 22] — which sets  $g_L = g_R$ . Both D-parity and  $SU(2)_R$  are broken during the descent of the GUT to the standard model, the first making the coupling constants unequal and the second resulting in a massive  $W_R$ . The possibility that the energy scale of breaking of D-parity is different from that of  $SU(2)_R$  breaking is admissible and well-examined [23]. The difference between these scales and the particle content of the theory controls the extent to which  $g_L \neq g_R$ .

<sup>1</sup>Earlier searches at the LHC for the  $W_R$  can be found in [9–12].

<sup>2</sup>The existence of three right-handed neutrinos —  $N_e, N_\mu$  and  $N_\tau$  — is acknowledged.

In this work we consider the different options of SO(10) symmetry breaking. It is shown that a light  $W_R$  goes hand-in-hand with the breaking of D-parity at a scale around  $10^{16}$  GeV, immediately excluding the possibility of  $g_L = g_R$ . D-parity breaking at such an energy is usually considered a desirable feature for getting rid of unwanted topological defects such as domain walls [24] and accounting for the baryon asymmetry of the Universe [25]. The other symmetries that are broken in the passage to the standard model are the  $SU(4)_C$  and  $SU(2)_R$  of the Pati-Salam (PS) model. The stepwise breaking of these symmetries and the order of their energy scales have many variants. There are also a variety of options for the scalar multiplets which are used to trigger the spontaneous symmetry breaking at the different stages. We take a minimalist position of (a) not including any scalar fields beyond the ones that are essential for symmetry breaking, and also (b) impose the Extended Survival Hypothesis (ESH) corresponding to minimal fine-tuning to keep no light extra scalars. With these twin requirements we observe that only a single symmetry-breaking route — the one in which the order of symmetry breaking is first D-parity, then  $SU(4)_C$ , and finally  $SU(2)_R$  — can accommodate a light  $M_{W_R}$ . We find that one must have  $0.64 \leq g_R/g_L \leq 0.78$ .

The paper is divided as follows. In the following section we give details of the CMS result [8] which are relevant for our discussion within the context of the left-right symmetric model. In the next section we elaborate on the GUT symmetry-breaking chains, the extended survival hypothesis for light scalars, and coupling constant evolution relations. Next we briefly note the implications of coupling constant unification within the Pati-Salam and SO(10) models. The results which emerge for the different routes of descent of SO(10) to the SM are presented in the next two sections. We end with our conclusions.

## 2 CMS $W_R$ search result and the left-right symmetric model

The results of the CMS collaboration for the search for a  $W_R$ -boson that we use [8] are based on the LHC run at  $\sqrt{s} = 8$  TeV with an integrated luminosity of  $19.7 \text{ fb}^{-1}$ . The focus is on the production of a  $W_R$  which then decays to a charged lepton ( $l$ ) and a right-handed heavy neutrino ( $N_l$ ), both of which are on-shell. The  $N_l$  undergoes a three-body decay to a charged lepton ( $l$ ) and a pair of quarks which manifest as hadronic jets ( $2j$ ), the process being mediated by a  $W_R$ . CMS examines the  $(2l)(2j)$  data within the framework of an LRS model with  $g_L = g_R$  and presents exclusion regions in the  $M_{W_R} - M_{N_l}$  plane.<sup>3</sup> Interpreting the four-object final state mass as that of a  $W_R$  CMS presents, in the supplementary material of [8], the 95% CL exclusion limits for the observed and expected  $\sigma(pp \rightarrow W_R) \times BR(W_R \rightarrow lljj) \equiv \sigma BR$  as functions of  $M_{W_R}$  for several  $M_{N_l}$ . From the data [8] one finds that in the electron channel, irrespective of the value of  $r = \frac{M_{N_e}}{M_{W_R}}$ ,  $\sigma BR_O$  (observed) exceeds twice the expected exclusion limit ( $\sigma BR_E$ ) for  $1.8 \lesssim M_{W_R} \lesssim 2.4$  TeV. This excess is about  $\sim 2.8\sigma$  around 2.1 TeV. Though not large enough for a firm conclusion, this can be taken as a tentative hint for a  $W_R$ , and if this is correct, one can expect confirmation in the new run of the LHC at  $\sqrt{s} = 13$  TeV. The CMS collaboration notes that this excess is not consistent with the LRS model with  $g_L = g_R$ ,  $r = 0.5$  and no leptonic

---

<sup>3</sup>An alternate explanation of the excess in the data could be in terms of a charged Higgs boson of the LRS model.

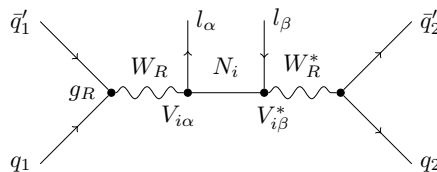


**Figure 1.** Feynman diagram of the process under discussion with the right-handed CKM-like mixing matrix taken in a general, non-diagonal, form. The CMS excess corresponds to  $l_\alpha = l_\beta = e$ .

mixing. As we stress later, relaxing these conditions — e.g.,  $r = 0.5$  — can make the results agree with the left-right symmetric model. No such excess is seen in the  $(2\mu)(2j)$  mode.

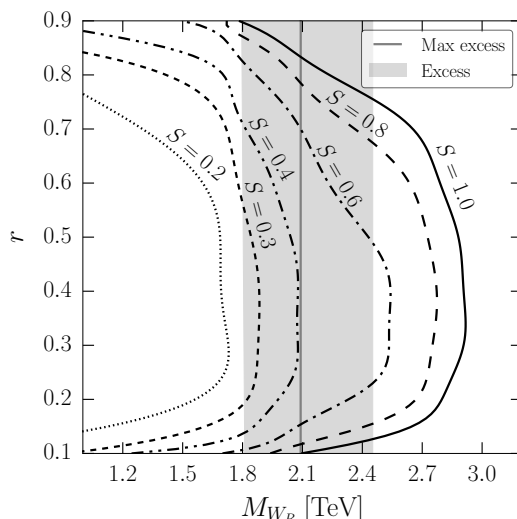
### 2.1 A $W_R$ signal?

Figure 1 shows the Feynman diagram for  $W_R$  production and its decay in the channels under consideration [26]. Note that the production of the  $W_R$  will be suppressed compared to that of a left-handed  $W$  boson of the same mass by a factor  $\eta^2$ , where  $\eta = (g_R/g_L)$ . The contribution from this diagram is determined by  $S^2$  where  $S \equiv \eta|V_{N_e e}|^2$ . Neglecting the masses of the final state quarks and the charged lepton, the branching ratio of the three-body decay of  $N_e$ , which we have calculated, is proportional to  $(1 - r^2)^2(2 + r^2)$ , where, as noted earlier,  $r = M_{N_e}/M_{W_R}$ . A clinching evidence of this process would then be a peak in the  $(2e)(2j)$  invariant mass at  $M_{W_R}$  — for which there is already a hint — along with another around  $M_{N_e}$  in the invariant mass of one of the two  $e(2j)$  combinations in every event. The absence of the latter in the data could be indicative of more than one  $N_R$  state being involved and further the coupling of these neutrinos to a  $\tau$ -lepton with non-negligible strength [13, 14, 27]. Subsequent leptonic decays of the  $\tau$  would mimic a dilepton signal but with two missed neutrinos washing out the expected  $e(2j)$  peak.

It has to be borne in mind that the excess seen in the  $(2e)(2j)$  mode is not matched in the  $(2\mu)(2j)$  data. This would have to be interpreted as an indication that the right-handed neutrino associated with the muon,  $N_\mu$ , is significantly heavier than  $N_e$  and so its production in  $W_R$ -decay suffers a large kinematic suppression. Further, the coupling of  $N_e$  to  $\mu$  has to be small, i.e.,  $|V_{N_e \mu}| \ll 1$ .

Interpretation of the excess in terms of  $N_e$ , a Majorana neutrino, would lead to the expectation of roughly an equal number of like-sign and unlike-sign dilepton events. There are fourteen events in the excess region in the CMS data in the  $(2e)(2j)$  channel, of which only one has charged leptons of the same sign. In a similar analysis by the ATLAS collaboration no like-sign events are found [28]. One way around this is to assume that two degenerate right-handed neutrinos together form a pseudo-Dirac state in which case the like-sign events are suppressed [18].

In figure 2 we place the excess observed by CMS in this channel — the shaded region in the  $M_{W_R} - r$  plane — in comparison with the LRS model predictions. This excess is maximum along the vertical line. The expectations from the Left-Right Symmetric model ( $\sigma BR_T$ ) depend on  $S^2 = \eta^2|V_{N_e e}|^4$  and  $r = M_{N_e}/M_{W_R}$ . The dashed curves in the figure, identified by the values of  $S$ , trace the points in the  $(r - M_{W_R})$  plane for which the LRS ex-



**Figure 2.** The shaded region demarcates the range of  $M_{W_R}$  for which the CMS data exceed twice the SM expectation. The maximum excess is on the vertical straight line. The curves parametrised by  $S \equiv \eta|V_{N_e e}|^2$  denote the  $(r, M_{W_R})$  contours for which the prediction of the LRS model is compatible with the observation.

expectations equal  $\sigma BR_O$ . To put the plot in context note that CMS has stressed [8] that with  $\eta = 1$  and  $V_{N_e} = 1$  — i.e.,  $S = 1$  — the LRS model signal for  $r = 0.5$  is inconsistent with the excess. This is borne out from figure 2 which indicates that for the  $S = 1$  contour, the  $M_{W_R}$  corresponding to  $r = 0.5$  lies outside the excess region. Consistency of the excess in the data with the LRS model can be accomplished in three ways. Firstly, if  $r = M_{N_e}/M_{W_R}$  is larger than 0.5 the LRS model signal will be reduced. Indeed, with  $r > 0.75$  the LRS model is consistent with the excess even with  $S = 1$ . Alternatively, if  $\eta$  or  $V_{N_e}$  is less than unity, then too the signal will be less, the suppression being determined by  $S^2$ . In figure 2 it can be seen that for  $r = 0.5$  the excess is consistent with the model for  $0.3 \lesssim S \lesssim 0.6$ . The upper limit has been pointed out in [15–17]. What we essentially find is that there are large sets of values of  $r$ ,  $\eta$  and  $V_{N_e}$  for which the LRS expectation is consistent with the excess.

Figure 2 contains information in a somewhat condensed form. In the spirit of the path chosen by the CMS collaboration, we use the exclusion data and plot in the left panel of figure 3  $\sigma BR_E$  (red dotted curve) and  $\sigma BR_O$  (blue dashed curve) as functions of  $M_{W_R}$  for the fixed value of  $r = 0.8$ . The prediction of the LRS model with  $\eta = g_R/g_L = 1$  and  $V_{N_e e} = 1$  is the black solid straight line. Also shown are the  $\pm 50\%$  (green, dark) and  $\pm 100\%$  (yellow, light) bands of the expected cross section. In the inset the same results are presented but for  $r = 0.5$ . Notice that for  $r = 0.8$  the LRS model expectation passes right through the maximum of the excess while for  $r = 0.5$  it entirely misses the excess region.

The right panel of figure 3 utilises a complementary way of displaying the region in the LRS model parameter space consistent with the result. Here the area in the  $\eta - V_{N_e e}$  plane that fits the CMS excess region is shown shaded for two values of  $r = 0.8$  (violet, dark) and 0.5 (green, light). Note that there is an overlap region. It is worth stressing that, as

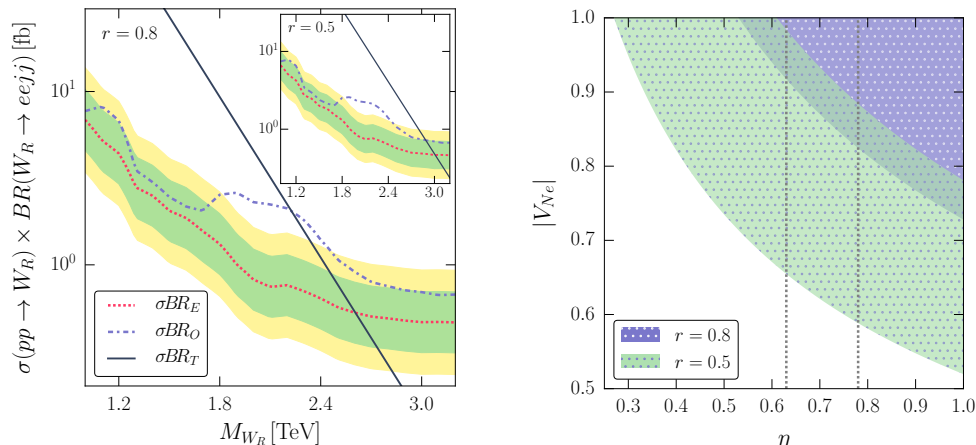


**Figure 3.** Left: the CMS data compared with the LRS model predictions for  $r = 0.8$  keeping  $g_R/g_L = 1$  and  $V_{Ne} = 1$ . Inset:  $r = 0.5$ . Right:  $\eta$  and  $V_{Ne}$  that fits the excess in the CMS data for  $r = 0.5$  and  $r=0.8$ . Only the region between the two vertical lines is permitted in SO(10) GUTs.

in the left panel, for  $r = 0.8$  the model is consistent with the data even for  $\eta = 1$  and  $V_{Ne} = 1$ . For  $r = 0.5$  a suppression through the factor  $S = \eta|V_{Ne}|^2$  is required to bring the model in harmony with the data. If the  $W_R$  with a mass  $\mathcal{O}(\text{TeV})$  arises from the SO(10) GUT model we discuss below then  $\eta$  must lie within the two vertical lines.

### 3 SO(10) grand unification

SO(10) is an attractive candidate for a unified theory [6, 7] as it is the simplest Lie group which includes all the SM fermions and a right-handed neutrino of one generation in a single irreducible representation. We do not include any exotic fermions in the model and deal with three generations.

There are a vast number of models characterised by different intermediate symmetries which have SO(10) as the unifying group. In that respect SO(10) is more of an umbrella term, incorporating these different models with alternate symmetry-breaking routes, scalar structures, and physics consequences. What is important for this work is that SO(10) has the Pati-Salam symmetry ( $\mathcal{G}_{PS}$ ) as a subgroup<sup>4</sup> and includes the discrete D-parity [21, 22] which enforces left-right parity,  $g_L = g_R$ . The Left-Right Symmetric group is embedded in  $\mathcal{G}_{PS}$ . Thus, having reviewed the CMS result in terms of the LRS model, both with and without left-right parity, the obvious next step is to look at it through the lenses of the Pati-Salam partial unified and SO(10) grand unified theories.

In this section we summarize the features of SO(10) GUTs which are relevant for our subsequent discussions. We consider the non-supersymmetric version of this theory.

#### 3.1 Symmetry breaking

The different ways in which SO(10) GUT can step-wise break to the SM are graphically represented in figure 4. The intermediate energy scales of various stages of symmetry

<sup>4</sup>SO(10) can break into  $\mathcal{G}_{SM}$  through two distinct routes, one through an intermediate SU(5) with no left-right symmetry and another through the PS stage. A longer proton decay lifetime  $\tau_p$  than predicted by minimal SU(5) and the ease of incorporation of seesaw neutrino masses give the second option a slight preference.

Symmetry	SO(10)	D-Parity	SU(4) <sub>C</sub>	SU(2) <sub>R</sub>	U(1) <sub>R</sub> × U(1) <sub>B-L</sub>	SU(2) <sub>L</sub> × U(1) <sub>Y</sub>
Breaking Scale	$M_U$	$M_D$	$M_C$	$M_R$	$M_0$	$M_Z$

**Table 1.** The different scales at which subgroups of SO(10) get broken.

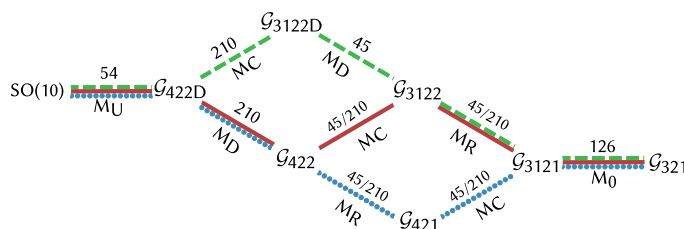


**Figure 4.** Symmetry breaking routes of SO(10) distinguished by the order of breaking of SU(2)<sub>R</sub>, SU(4)<sub>C</sub>, and D-parity. The scalar multiplets responsible for symmetry breaking at every stage have been indicated. Only the DCR (red solid) route can accommodate the light  $W_R$  scenario.

breaking will be denoted according to table 1. Among these,  $M_D \geq M_R \geq M_0 > M_Z$  always. In order to systematically study the different ways in which SO(10) can descend to the SM, we first classify them into *routes* based on the order of symmetry breaking. We will call the route with  $M_C \geq M_D \geq M_R$ , CDR (Green, Dashed), the one with  $M_D \geq M_C \geq M_R$ , DCR (Red, Solid), and another, DRC (Blue, Dotted), with  $M_D \geq M_R \geq M_C$ . Thus there are three alternate routes with a maximum number of four intermediate stages. Among the intermediate stages the first and the last, namely, SU(4)<sub>C</sub> × (SU(2)<sub>L</sub> × SU(2)<sub>R</sub>)<sub>D</sub> ( $\equiv \mathcal{G}_{422D}$ ) and SU(3)<sub>C</sub> × U(1)<sub>B-L</sub> × SU(2)<sub>L</sub> × U(1)<sub>R</sub> ( $\equiv \mathcal{G}_{3121}$ ), are common to all routes. The other possible intermediate symmetries, in this notation, are  $\mathcal{G}_{422}$ ,  $\mathcal{G}_{421}$ ,  $\mathcal{G}_{3122D}$ , and  $\mathcal{G}_{3122}$  (see figure 4). All models of SO(10) symmetry breaking (symmetry-breaking *chains*) are thus defined by the route it belongs to and the Higgs multiplets that it includes. Figure 4 shows the *maximum-step chains* (chains with maximum number of intermediate symmetries) of each route. Other chains are essentially subcases of these with multiple symmetries breaking at the same scale. This can be achieved if multiple Higgs sub-multiplets gain vacuum expectation value (*vev*) at the same scale or if a single sub-multiplet breaks more than one symmetry.

### 3.2 Scalar structure and the Extended Survival Hypothesis (ESH)

The gauge bosons in the model and their masses are determined by the symmetry group and its sequential breaking to the SM. The fermions come in three generations in each of which there are the SM quarks and leptons and a right-handed neutrino. Thus it is only the scalar sector which retains a degree of flexibility.

The generation of quark and lepton masses requires a 10 of SO(10) while the see-saw mechanism for neutrino masses relies on a 126. Their decompositions under the PS group

are:<sup>5</sup>

$$10 = [1, 2, 2] + [6, 1, 1], \tag{3.1}$$

and

$$126 = [6, 1, 1] + [15, 2, 2] + [10, 3, 1] + [\overline{10}, 1, 3]. \tag{3.2}$$

These scalars also have important roles in gauge symmetry breakings. The *vev* of the 10, which is  $\mathcal{O}(M_Z)$ , breaks the standard model  $SU(2)_L \times U(1)_Y$  symmetry while the 126 is responsible for the breaking of  $U(1)_{B-L} \times U(1)_R$  at the scale  $M_0$ .

In a grand unified theory masses of fermions in the same multiplet are related. In particular, the 10 of  $SO(10)$  implies  $M_d = M_l^\dagger$ , where  $M_d$  is the mass matrix of  $d$ -type quarks and  $M_l$  that of the charged leptons. Though these relations are valid only at the scale of unification and at lower energies corrections have to be included, even then they are not in consistency with the measured masses. One way to address this issue is to invoke a  $[15, 2, 2]$  submultiplet which is present in the 126 and the 120 of  $SO(10)$  to bring the masses closer to their actual values [29, 30].

Two other  $SO(10)$  representations which turn out to be useful for symmetry breaking and whose submultiplet structure will be important are the 45 and 210. Under the PS group they consist of:

$$45 = [15, 1, 1] + [6, 2, 2] + [1, 3, 1] + [1, 1, 3], \tag{3.3}$$

$$210 = [1, 1, 1] + [15, 1, 1] + [6, 2, 2] + [15, 3, 1] + [15, 1, 3] + [10, 2, 2] + [\overline{10}, 2, 2]. \tag{3.4}$$

Even using these limited  $SO(10)$  multiplets,<sup>6</sup> there remains a variety of options for the scalar submultiplets that can be used for the different stages of symmetry breaking indicated in figure 4. They affect the unification and intermediate energy scales through their role in the evolution of gauge couplings. We make two restrictions: (a) Only renormalisable terms will be kept in the  $SO(10)$ -symmetric lagrangian,<sup>7</sup> and (b) The Extended Survival Hypothesis, which is a consequence of minimal fine-tuning, is taken to be valid.

According to ESH [31, 32], at any intermediate energy scale only those scalar submultiplets (under the unbroken symmetry at that stage) which are required to spontaneously break a symmetry at that or any lower energy remain massless. All other submultiplets become massive. Because the normal expectation of scalar masses is to be at the highest energy scale the extended survival hypothesis posits the minimal number of fine-tunings in the scalar sector.

With these guiding principles we now turn to the scalar multiplets that are employed for the descent of  $SO(10)$  to the SM. The first (at  $M_U$ ) and last (at  $M_0$ ) stages of the symmetry breaking in figure 4, which are common to all alternate channels, utilise a 54-plet and a 126-plet of scalar fields, respectively. D-parity is broken through the *vev* of

---

<sup>5</sup>We will use the notation  $[\phi_4, \phi_L, \phi_R]$  to specify the behaviour of  $SO(10)$  submultiplets under the Pati-Salam symmetry.

<sup>6</sup>A 54 is used for the first step of GUT symmetry breaking. It does not affect the RG running of the couplings.

<sup>7</sup>This excludes, for example, using scalar 16-plets to mimic the  $SO(10)$  126 for neutrino mass through effective dimension-5 terms in the Lagrangian.

D-odd scalars. There is a D-odd PS singlet in the  $\underline{210}$  of  $SO(10)$  which can be utilised for the DCR or DRC symmetry-breaking route. For the CDR route a D-odd LRS model singlet in the  $[15,1,1]$  of  $\underline{45}$  is useful.

### 3.3 Renormalisation group equations

The one-loop RG evolution for the coupling  $\alpha^g(\mu)$  corresponding to a gauge symmetry  $g$  can be written as:

$$\frac{1}{\alpha^g(\mu_i)} = \frac{1}{\alpha^g(\mu_j)} + \frac{b_{ji}^g}{2\pi} \ln\left(\frac{\mu_j}{\mu_i}\right). \quad (3.5)$$

$b_{ji}^g$  is the coefficient of the  $\beta$ -function between the scales  $\mu_i$  and  $\mu_j$ :

$$b^g = -\frac{11}{3}N_g + \frac{2}{3} \sum_F T(F_g)d(F_{g'})n_G + \frac{1}{6} \sum_S \delta_S T(S_g)d(S_{g'}), \quad (3.6)$$

where the three terms are contributions from gauge bosons, chiral fermions, and scalars respectively.  $N_g$  is the quadratic Casimir corresponding to the particular symmetry group  $g$ ,  $N_g$  is 0 for  $U(1)$  and  $N$  for  $SU(N)$ .  $T(F_g)$  and  $d(F_g)$  are the index and the dimension of the representation of the chiral fermion multiplet  $F$  under the group  $g$  and the sum is over all fermion multiplets of one generation.  $n_G$  is the number of fermion generations, 3 in our case. Similarly  $T(S_g)$  and  $d(S_g)$  are the index and the dimension of the representation  $S_g$  of the scalar  $S$  under  $g$ .  $\delta_S$  takes the value 1 or 2 depending on whether the scalar representation is real or complex.

It is worth noting that  $b^g$  is positive for  $U(1)$  subgroups and negative<sup>8</sup> for  $SU(n)$ . Therefore,  $U(1)$  couplings grow with increasing energy while  $SU(n)$  couplings decrease.

For ease of use, we will rewrite eq. (3.5) as:

$$w_i^g = w_j^g + \frac{1}{2\pi} b_{ji}^g \Delta_{ji}, \quad (3.7)$$

where  $w_i^g \equiv \frac{1}{\alpha^g(\mu_i)}$  and  $\Delta_{ji} \equiv \ln\left(\frac{\mu_j}{\mu_i}\right)$ .

If the symmetry  $g$  is broken to  $g'$  at the scale  $\mu_i$  then the coupling constant matching condition is simply  $w_i^g = w_i^{g'}$  unless two groups combine to yield a residual symmetry. As an example of the latter, for  $U(1)_Y$  of the standard model, resulting from a linear combination of  $U(1)_R$  and  $U(1)_{B-L}$  at the scale  $M_0$ , one has:

$$w_0^Y = \frac{3}{5}w_0^R + \frac{2}{5}w_0^{B-L}. \quad (3.8)$$

Matching all the couplings at the boundaries and imposing the unification condition one arrives at three equations:

$$w_Z^3 = w_U + \frac{1}{2\pi} \sum_i b_{i,i-1}^C \Delta_{i,i-1},$$

---

<sup>8</sup>Contributions from large scalar multiplets can make the beta-function positive. This does happen for  $SU(2)_R$  in the example we discuss later.

$$\begin{aligned}
 w_Z^{2L} &= w_U + \frac{1}{2\pi} \sum_i b_{i,i-1}^{2L} \Delta_{i,i-1}, \\
 w_Z^Y &= w_U + \frac{3}{5} \frac{1}{2\pi} \sum_i b_{i,i-1}^{1R} \Delta_{i,i-1} + \frac{2}{5} \frac{1}{2\pi} \sum_i b_{i,i-1}^{B-L} \Delta_{i,i-1},
 \end{aligned}
 \tag{3.9}$$

where  $w_U$  is the reciprocal of the coupling strength at unification.  $i$  runs from the unification scale to  $M_0$ .  $C$  stands for  $SU(3)_C$  or  $SU(4)_C$  depending on the energy scale  $\mu$ . Similarly,  $1R$  ( $B-L$ ) in the last equation represents  $U(1)_R$  or  $SU(2)_R$  ( $U(1)_{B-L}$  or  $SU(4)_C$ ).

The left-hand-sides of the three equations in (3.9) are the inputs fixed by experiments. The equations are linear in  $w_U$  and  $\ln(\mu_i)$  — the logarithms of the mass-scales. There are  $2+m$  variables:  $m$ , the number of scales intermediate to  $M_U$  and  $M_Z$ ,  $w_U$ , the magnitude of the coupling at unification, and the GUT scale  $M_U$  itself. Thus, an  $SO(10)$  chain with one intermediate scale ( $m = 1$ ) is a determined system while those with more steps are underdetermined.

## 4 Low energy expectations from unification

In the LRS model the energy scales of symmetry breaking can be freely chosen to be consistent with the low energy data. Once embedded in GUTs one must also verify that such choices of intermediate scales are consistent with perturbative unification of the couplings at sub-Planck energies and check their implications for other symmetry-breaking scales. In this section we look at the restrictions imposed by coupling unification on  $\eta$  and the other left-right symmetric model parameters.

$SO(10)$  can descend to the SM through a maximum of four intermediate stages (figure 4). Such four-step symmetry breakings are underdetermined. Accordingly, one is permitted to choose the scale  $M_R$  in the TeV range, as required by the CMS data, and to check the consistency of the equations.  $M_0$  is always below  $M_R$  and thus keeping the latter at a few TeV sets the former to an even lower value.

### 4.1 Pati-Salam partial unification

The PS symmetry with D-parity,  $\mathcal{G}_{422D}$ , is a common intermediate stage for all the  $SO(10)$  symmetry-breaking options. When D-parity is intact, this model has two-independent couplings, namely,  $g_{4C}$  and  $g_{2L} = g_{2R} = g_2$ , which achieve equality at the grand unification scale  $M_U$ . In the DCR route the Pati-Salam  $\mathcal{G}_{422}$  survives at the next step but D-parity no longer holds. In contrast, for the CDR chain the PS symmetry is broken before D-parity. Needless to say, so long as D-parity remains unbroken  $\eta = 1$ .

In Pati-Salam partial unification one has a set of three equations similar to eq. (3.9) sans the constraint of grand unification. In place of an inverse GUT coupling  $w_U$  one gets two separate couplings —  $w_C^4$  ( $= w_C^{B-L} = w_C^3$ ) at  $M_C$  and  $w_D^2$  ( $= w_D^{2R} = w_D^{2L}$ ) at  $M_D$ . Thus, the two variables — the GUT coupling and the GUT scale — are replaced by the  $SU(4)_C$  unification coupling and a D-parity symmetric  $SU(2)$  coupling. In the following sections we will look at the results that arise from RG evolution for both PS partial unification and  $SO(10)$  grand unification.

## 4.2 Left-right symmetry and unification

The scalar field contributions to gauge coupling evolution play a significant role in achieving coupling unification while keeping a low  $M_R$ . This has led to a plethora of models where scalar fields have been incorporated in the theory solely for this purpose. This is not the path that we choose. Indeed, the scalar fields which we *do* include become indispensable in some cases. For example, a subcase which one might imagine from figure 4 will have  $M_R = M_0$ . The one-step symmetry breaking of  $\mathcal{G}_{3122} \rightarrow \mathcal{G}_{321}$  can be realized through the *vev* of just a  $[\overline{10}, 1, 3] \subset \underline{126}$ , dispensing off the submultiplet which breaks  $SU(2)_R \rightarrow U(1)_R$ . However, without this latter contribution the coupling constants no longer unify. So,  $M_R = M_0 \sim \mathcal{O}(\text{TeV})$  cannot be accommodated without at least the scalar multiplets that we keep.

As mentioned earlier, the three key ingredients in interpreting the CMS result are the ratio between the left- and right-handed gauge couplings,  $\eta$ , the Majorana mass of the right-handed electron neutrino,  $M_{N_e}$ , and the right-handed leptonic mixing  $V_{Nl}$ . The Majorana mass of the right-handed neutrino of the  $l$ -th flavour, in the TeV range, is obtained through the Yukawa coupling  $Y_{126}^l$ . The mass is proportional to the  $\Delta L = 2$  *vev*,  $v_{126}$ , of the  $(1, -2, 1, 1) \subset [\overline{10}, 1, 3] \subset \underline{126}$ . The latter also breaks the  $\mathcal{G}_{3121}$  symmetry. Hence, one has  $M_{N_l} \sim (Y_{126}^l/g_{B-L})M_0$ . The Yukawa coupling,  $Y_{126}^l$ , can be chosen to obtain a desired value of  $M_{N_l}$  without affecting other physics. Thus the choice of  $r = M_N/M_{W_R}$  is decoupled from the analysis of coupling unification.

The mixing in the right-handed lepton sector —  $V_{Nl}$  — is the second relevant quantity in this analysis. It is determined by the generation structure of the Yukawa matrix. Since this does not affect the evolution of couplings, which is the focus, our analysis does not impose any restriction on the choice of this mixing.

The relative strength of the right-handed coupling *vis-à-vis* the left-handed one at the  $SU(2)_R$ -breaking scale —  $\eta = \frac{g_R}{g_L}$  — is, however, intimately related to the RG running of the gauge couplings.

$$w_R^{2R} = \frac{1}{\eta^2} w_R^{2L}. \tag{4.1}$$

The magnitude of  $\eta$  will vary for symmetry-breaking chains depending on the scalar content of the theory and the energy scales at which different symmetries break. Nonetheless, the minimum value that can be attained by  $\eta$  is almost independent of the way in which  $SO(10)$  or  $\mathcal{G}_{PS}$  descends to the standard model, as we now discuss. Firstly the requirement that  $M_R$  is  $\mathcal{O}(\text{TeV})$  and  $M_0$  even lower, keeps them close to each other and the two are not too far from  $M_Z$  either. The other feature, noted earlier, is that  $U(1)$  couplings increase as the energy scale  $\mu$  increases while  $SU(n)$  couplings do the opposite.

One starts from eq. (3.8) which relates the  $U(1)$  couplings when the symmetry breaking  $\mathcal{G}_{3121} \rightarrow \mathcal{G}_{321}$  occurs at  $M_0$ . Obviously,

$$w_0^{1R} > w_R^{1R} = w_R^{2R} = \left(\frac{1}{\eta^2}\right) w_R^{2L}, \tag{4.2}$$

and from  $w_C^{B-L} = w_C^{3C}$

$$w_0^{B-L} > w_R^{B-L} > w_R^{3C}. \tag{4.3}$$

From eq. (3.8) together with eqs. (4.2) and (4.3) one has

$$\eta^2 > \frac{3w_R^{2L}}{5w_0^Y - 2w_R^{3C}} \simeq \frac{3w_0^{2L}}{5w_0^Y - 2w_0^{3C}}. \quad (4.4)$$

The inequality in the first step in eq. (4.2) is due to the evolution of  $w^{1R}$  from  $M_0$  to  $M_R$ . Since these two energy scales are both in the TeV range this effect is not large. A similar reasoning is also valid for the first inequality in eq. (4.3) but the second could be much more substantial. Using the current values of the low energy couplings<sup>9</sup> and extrapolating them to  $\mu = M_0$  one gets

$$\eta_{\min} \sim 0.59. \quad (4.5)$$

We stress that eq. (4.5) is an artefact of the LRS model so long as there is a merging of the  $U(1)_{B-L}$  with  $SU(3)_C$ , and so is valid for both PS (partial) and SO(10) (grand) unification. However, this is a limit in principle, accomplishing it will depend on the details of symmetry breaking and the scalar content of the theory. We have previously seen that if  $r = 0.5$  the CMS result is compatible with the LRS model for  $S$  as low as  $\sim 0.25$ . From the preceding discussion we see that  $S$  lower than  $\sim 0.59$  cannot be attained by  $\eta$  alone.

## 5 The three routes of SO(10) symmetry breaking

In this section we consider one by one the three routes depicted in figure 4 by which SO(10) can descend to the SM. We focus on the scalar fields that are required and the intermediate energy scales involved. We use one-loop renormalisation group equations here but have checked that two-loop effects — on which we comment later on — do not change the results drastically. Since the equations are usually underdetermined, motivated by the CMS data, we will keep  $4 \text{ TeV} \leq M_R \leq 10 \text{ TeV}$  and  $1 \text{ TeV} \leq M_0 \leq 4 \text{ TeV}$  for the chains of descent.

### 5.1 The DRC route

Restricting  $M_R$  to the TeV range automatically eliminates the DRC route (Blue dotted in figure 4) —  $SU(4)_C$  breaking *after*  $M_R$  — because then the leptoquark gauge bosons of  $SU(4)_C$  achieve a mass of the TeV order. Light leptoquarks below  $10^6 \text{ GeV}$  are forbidden from rare decays of strange mesons, such as  $K_L \rightarrow \mu e$  [2, 34, 35]. The DRC route of symmetry breaking is thus not compatible with the CMS result.

### 5.2 The CDR route

With all intermediate stages distinct, for this route (Green dashed in figure 4) one has:

$$SO(10) \xrightarrow{\frac{M_U}{54}} \mathcal{G}_{422D} \xrightarrow{\frac{M_C}{210}} \mathcal{G}_{3122D} \xrightarrow{\frac{M_D}{210}} \mathcal{G}_{3122} \xrightarrow{\frac{M_R}{210}} \mathcal{G}_{3121} \xrightarrow{\frac{M_0}{126}} \mathcal{G}_{321}. \quad (5.1)$$

The scalar submultiplets responsible for the symmetry breaking are shown in table 2. An alternative to the above would be to break  $\mathcal{G}_{3122} \rightarrow \mathcal{G}_{3121}$  using a  $[1,1,3] \subset \underline{45}$  in place of the  $[15, 1, 3] \subset \underline{210}$ . We also comment about this option.

<sup>9</sup>We use  $\alpha_3 = 0.1185(6)$ ,  $\sin^2 \theta_W = 0.23126(5)$ , and  $\alpha = 1/127.916$  at  $\mu = M_Z$  [33].

SO(10) repn.	Symmetry breaking	Scalars contributing to RG				
		$M_Z \leftrightarrow M_0$	$M_0 \leftrightarrow M_R$	$M_R \leftrightarrow M_D$	$M_D \leftrightarrow M_C$	$M_C \leftrightarrow M_U$
		$\mathcal{G}_{321}$	$\mathcal{G}_{3121}$	$\mathcal{G}_{3122}$	$\mathcal{G}_{3122D}$	$\mathcal{G}_{422D}$
<b>10</b>	$\mathcal{G}_{321} \rightarrow EM$	(1,2, $\pm 1$ )	(1,0,2, $\pm \frac{1}{2}$ )	(1,0,2,2)	(1,0,2,2) <sub>+</sub>	[1,2,2] <sub>+</sub>
<b>126</b>	$\mathcal{G}_{3121} \rightarrow \mathcal{G}_{321}$	-	(1,-2,1,1)	(1,-2,1,3)	(1,-2,1,3) <sub>+</sub>	$[\overline{10},1,3]$ <sub>+</sub>
		-	-	-	(1,2,3,1) <sub>+</sub>	[10,3,1] <sub>+</sub>
<b>210</b>	$\mathcal{G}_{3122} \rightarrow \mathcal{G}_{3121}$	-	-	(1,0,1,3)	(1,0,1,3) <sub>+</sub>	[15,1,3] <sub>+</sub>
		-	-	-	(1,0,3,1) <sub>+</sub>	[15,3,1] <sub>+</sub>
<b>210</b>	$\mathcal{G}_{3122D} \rightarrow \mathcal{G}_{3122}$	-	-	-	(1,0,1,1) <sub>-</sub>	[1,1,1] <sub>-</sub>
<b>210</b>	$\mathcal{G}_{422D} \rightarrow \mathcal{G}_{3122D}$	-	-	-	-	[15,1,1] <sub>+</sub>

**Table 2.** Scalar fields considered when the ordering of symmetry-breaking scales is  $M_C \geq M_D \geq M_R$ . The submultiplets contributing to the RG evolution at different stages according to the ESH are shown. D-parity ( $\pm$ ) is indicated as a subscript.

In order to proceed with an elaboration of the consequences associated with this route it is helpful to list the one-loop beta-function coefficients for the stages  $M_R \leftrightarrow M_D$  and  $M_D \leftrightarrow M_C$ . Including the contributions from the scalars in table 2, fermions, and gauge bosons one finds from eq. (3.5)

$$\begin{aligned}
 b_{DR}^3 &= -7, & b_{DR}^{B-L} &= \frac{11}{2}, & b_{DR}^{2L} &= -3, & b_{DR}^{2R} &= -2, \\
 b_{CD}^3 &= -7, & b_{CD}^{B-L} &= 7, & b_{CD}^{2L} &= -2, & b_{CD}^{2R} &= -2.
 \end{aligned}
 \tag{5.2}$$

The  $SU(2)_L$  and  $SU(2)_R$  couplings evolve from  $M_R$  to become equal at  $M_D$ . This requires ( $\Delta_{AB} = \ln \frac{M_A}{M_B}$ ):

$$w_R^{2L} - w_R^{2R} = \frac{1}{2\pi} \{ (b_{DR}^{2L} - b_{DR}^{2R}) \Delta_{DR} \}.
 \tag{5.3}$$

Similarly the  $SU(3)_C$  and  $U(1)_{B-L}$  couplings become equal at  $M_C$ , i.e.,

$$w_R^3 - w_R^{B-L} = \frac{1}{2\pi} \{ (b_{DR}^3 - b_{DR}^{B-L}) \Delta_{DR} + (b_{CD}^3 - b_{CD}^{B-L}) \Delta_{CD} \}.
 \tag{5.4}$$

The left-hand-sides of eqs. (5.3) and (5.4) are given in terms of the various couplings at  $M_R$ . Since  $M_R \sim \mathcal{O}(\text{TeV})$  and the RG evolution is logarithmic in energy it is not a bad approximation to assume that they do not change significantly from  $M_Z$  to  $M_R$ , i.e.,  $w_R^i \simeq w_O^i \simeq w_Z^i$ . Then recalling eq. (3.8) which relates  $w_0^Y$  with  $w_0^R$  and  $w_0^{B-L}$  one can obtain:

$$3w_Z^{2L} + 2w_Z^3 - 5w_Z^Y \simeq \frac{1}{2\pi} \{ [3(b_{DR}^{2L} - b_{DR}^{2R}) + 2(b_{DR}^3 - b_{DR}^{B-L})] \Delta_{DR} + 2(b_{CD}^3 - b_{CD}^{B-L}) \Delta_{CD} \}.
 \tag{5.5}$$

Using the beta-function coefficients from eq. (5.2), one can reexpress eq. (5.5) as:

$$3w_Z^{2L} + 2w_Z^3 - 5w_Z^Y \simeq \frac{1}{2\pi} \{ 28 \Delta_{CR} \}.
 \tag{5.6}$$

SO(10) repn.	Symmetry breaking	Scalars contributing to RG				
		$M_Z \leftrightarrow M_0$	$M_0 \leftrightarrow M_R$	$M_R \leftrightarrow M_C$	$M_C \leftrightarrow M_D$	$M_D \leftrightarrow M_U$
		$\mathcal{G}_{321}$	$\mathcal{G}_{3121}$	$\mathcal{G}_{3122}$	$\mathcal{G}_{422}$	$\mathcal{G}_{422D}$
<b>10</b>	$\mathcal{G}_{321} \rightarrow EM$	(1,2, $\pm 1$ )	(1,0,2, $\pm \frac{1}{2}$ )	(1,0,2,2)	[1,2,2]	[1,2,2] <sub>+</sub>
<b>126</b>	$\mathcal{G}_{3121} \rightarrow \mathcal{G}_{321}$	-	(1,-2,1,1)	(1,-2,1,3)	$[\overline{10},1,3]$	$[\overline{10},1,3]$ <sub>+</sub>
		-	-	-	-	$[10,3,1]$ <sub>+</sub>
<b>210</b>	$\mathcal{G}_{3122} \rightarrow \mathcal{G}_{3121}$	-	-	(1,0,1,3)	[15,1,3]	[15,1,3] <sub>+</sub>
		-	-	-	-	$[15,3,1]$ <sub>+</sub>
<b>210</b>	$\mathcal{G}_{422} \rightarrow \mathcal{G}_{3122}$	-	-	-	[15,1,1]	[15,1,1] <sub>+</sub>
<b>210</b>	$\mathcal{G}_{422D} \rightarrow \mathcal{G}_{422}$	-	-	-	-	[1,1,1] <sub>-</sub>

**Table 3.** Scalar fields considered when the ordering of symmetry-breaking scales is  $M_D \geq M_C \geq M_R$ . The submultiplets contributing to the RG evolution at different stages according to the ESH are shown. D-parity ( $\pm$ ) is indicated as a subscript.

Notice that  $M_D$  has dropped out. Further, the low energy values of  $\alpha, \alpha_s$  and  $\sin^2 \theta_W$  [33] then imply  $M_C \sim 10^{18} M_R$ , i.e., way beyond the Planck scale. The low energy SM parameters are now quite well-measured and offer no escape route from this impasse. Two-loop contributions also do not change the situation drastically. We have checked that if one breaks  $\mathcal{G}_{3122} \rightarrow \mathcal{G}_{3121}$  through a  $[1,1,3] \subset \underline{45}$  rather than the  $[15,1,3] \subset \underline{210}$  (see table 2), the change is in the evolution of the couplings in the  $M_C \leftrightarrow M_U$  sector which does not affect this conclusion.

The above analysis does not resort to the constraint of grand unification at all. The results hold for PS partial unification as well. So, the CDR route of descent also has to be abandoned for  $M_R \sim \mathcal{O}(\text{TeV})$ .

### 5.3 The DCR route

After having eliminated the other alternatives, the only remaining route of descent has the mass ordering  $M_D \geq M_C \geq M_R$  (Red solid in figure 4). Keeping all possible intermediate stages separate from each other this corresponds to:

$$\text{SO}(10) \xrightarrow[\substack{M_U \\ 54}]{\mathcal{G}_{422D}} \xrightarrow[\substack{M_D \\ 210}]{\mathcal{G}_{422}} \xrightarrow[\substack{M_C \\ 210}]{\mathcal{G}_{3122}} \xrightarrow[\substack{M_R \\ 210}]{\mathcal{G}_{3121}} \xrightarrow[\substack{M_0 \\ 126}]{\mathcal{G}_{321}}. \quad (5.7)$$

In the above we have indicated the SO(10) multiplets which contribute to symmetry breaking at every stage. The scalar submultiplets which contribute to the RG equations as dictated by ESH are shown in table 3. There is, however, an alternative which relies on a  $\underline{45}$  of SO(10) whose contents under the Pati-Salam group are given in eq. (3.3).  $\text{SU}(2)_R$  can be broken by the  $(1,0,1,3) \subset [1,1,3] \subset \underline{45}$  replacing the  $[15,1,3] \subset \underline{210}$ . In fact, the

$SU(4)_C$  breaking  $[15,1,1]$  is also present in the 45. However, one cannot entirely dispense with the 210 because the  $[1,1,1]_-$  in it has no analog in the 45.

Denoting by  $h_D, h_C, h_R$  the  $SO(10)$  scalar multiplets responsible for the breaking of D-Parity,  $SU(4)_C$ , and  $SU(2)_R$  respectively, we therefore have the following alternatives:  $\{h_D, h_C, h_R\}$  can be  $\{210, 45, 45\}$ ,  $\{210, 45, 210\}$ ,  $\{210, 210, 45\}$  and  $\{210, 210, 210\}$ . Of these, the first employs the lowest dimensional scalar multiplets required to break symmetries at each scale while the last one uses the least number of  $SO(10)$  scalar multiplets. Using 45 or 210 for  $h_C$  makes no difference in the physics since in both cases a  $[15,1,1]$  Pati-Salam submultiplet is used. The distinction is relevant only in the choice of  $h_R$ .

The one-loop beta-function coefficients for the couplings in the  $M_R \leftrightarrow M_C$  and  $M_C \leftrightarrow M_D$  energy ranges obtained using eq. (3.5) and the scalars in table 3 are:

$$\begin{aligned} b_{CR}^3 &= -7, & b_{CR}^{B-L} &= \frac{11}{2}, & b_{CR}^{2L} &= -3, & b_{CR}^{2R} &= -2, \\ b_{DC}^4 &= -5, & b_{DC}^{2L} &= -3, & b_{DC}^{2R} &= \frac{26}{3}. \end{aligned} \tag{5.8}$$

The  $SU(3)_C$  and  $U(1)_{B-L}$  couplings evolve to become equal at  $M_C$ . Thus

$$w_R^3 - w_R^{B-L} = \frac{1}{2\pi} \left\{ (b_{CR}^3 - b_{CR}^{B-L}) \Delta_{CR} \right\}. \tag{5.9}$$

Matching of the  $SU(2)_L$  and  $SU(2)_R$  couplings at  $M_D$  implies:

$$w_R^{2L} - w_R^{2R} = \frac{1}{2\pi} \left\{ (b_{CR}^{2L} - b_{CR}^{2R}) \Delta_{CR} + (b_{DC}^{2L} - b_{DC}^{2R}) \Delta_{DC} \right\}. \tag{5.10}$$

As before, we use the approximation  $w_R^i \simeq w_O^i \simeq w_Z^i$  and combine eqs. (5.9) and (5.10) to get:

$$3w_Z^{2L} + 2w_Z^3 - 5w_Z^Y \simeq \frac{1}{2\pi} \left\{ [3(b_{CR}^{2L} - b_{CR}^{2R}) + 2(b_{CR}^3 - b_{CR}^{B-L})] \Delta_{CR} + 3(b_{DC}^{2L} - b_{DC}^{2R}) \Delta_{DC} \right\}. \tag{5.11}$$

A special limit of the DCR route is when  $M_D = M_C$ , i.e.,  $\Delta_{DC} = \ln \frac{M_D}{M_C} = 0$ . In this limiting case there is no distinction between this route and the CDR one. Indeed, setting  $M_D = M_C$  in eq. (5.11) and substituting the beta-function coefficients from eq. (5.8) one exactly reproduces (5.6) which places the solution in an unacceptable energy regime.

That one should nonetheless expect acceptable solutions can be surmised from the fact that eq. (5.11) implies

$$\begin{aligned} \frac{d \ln M_C}{d \ln M_D} &= \frac{3(b_{DC}^{2L} - b_{DC}^{2R})}{[3(b_{DC}^{2L} - b_{DC}^{2R}) - b_{CR}^{2L} + b_{CR}^{2R}] - 2(b_{CR}^3 - b_{CR}^{B-L})} \\ &= 5, \end{aligned} \tag{5.12}$$

where in the last step we have used eq. (5.8). This indicates that  $M_C$  changes faster than  $M_D$  and so starting from the  $M_D = M_C$  limit solutions in the DCR route with the symmetry breaking scales below  $M_{\text{Planck}}$  are feasible. Replacing the 210 in  $h_R$  by a 45 reduces  $b_{DC}^{2R}$  so much that unification of couplings is no longer possible. In the next section we present the allowed solutions in detail.

## 6 SO(10) unification with $M_R \sim \mathcal{O}(\text{TeV})$

In the previous section we have seen that of the three routes of symmetry breaking accessible to SO(10), DRC is trivially eliminated when the twin requirements  $M_R \sim \mathcal{O}(\text{TeV})$  and  $M_R > M_C$  are imposed. We also indicated that for the CDR route with the minimal scalar content and following the extended survival hypothesis the requirement  $M_R \sim \mathcal{O}(\text{TeV})$  implies  $M_C > M_{\text{Planck}}$ . The only route that can accommodate  $M_R \sim \mathcal{O}(\text{TeV})$  is DCR.

To simplify the discussion, in eq. (5.11) we have ignored the running of the couplings between  $M_Z$  and  $M_R$ . In obtaining the results presented in this section we have not used such an approximation. We have, however, not included the effect of mixing of  $U(1)_R \times U(1)_{B-L}$  under RG evolution from  $M_0$  to  $M_R$ . As these two scales are close to each other, both in the few TeV range, the impact of the mixing will not be large.

### 6.1 Pati-Salam partial unification for the maximum-step case

The maximum-step symmetry-breaking DCR route has been given in eq. (5.7). Before turning to SO(10) we briefly remark about Pati-Salam partial unification within this route. Because there are four steps of symmetry breaking this is an underdetermined system. For this work,  $M_R$  is restricted to be in the  $\mathcal{O}(\text{TeV})$  range. The scale  $M_C$  is taken as the other input in the analysis. At the one-loop level the results can be analytically calculated using the beta-function coefficients in eq. (5.8). The steps can be identified from eqs. (5.10) and (5.11). The latter determines  $M_D$  once  $M_C$  is chosen.  $\eta$  is then fixed using eq. (5.10).

For example, for  $M_C = 10^6 \text{ GeV}$  one gets  $\eta = 0.63$  when  $M_R = 5 \text{ TeV}$ . Within the Pati-Salam model the upper limit of  $M_D$  is set by  $M_{\text{Planck}}$ . We find that in such a limit one has  $M_C = 10^{17.6} \text{ GeV}$  and  $\eta = 0.87$  for  $M_R = 5 \text{ TeV}$ .

### 6.2 Coupling unification for the maximum-step case

For SO(10) grand unification one must find the energy scale at which the common  $SU(2)_{L,R}$  coupling beyond  $M_D$  equals the  $SU(4)_C$  coupling, i.e.,  $g_2 = g_{4C}$ . This limits the upper bound of  $M_C$  compared to the Pati-Salam partial unification.

In the left panel of figure 5 we plot  $\eta$  as a function of  $M_C$ . In the inset is shown the behaviour of  $M_U$  and  $M_D$  as functions of  $M_C$ . Due to the unification constraint, the upper limits of  $M_C$ ,  $M_D$  and  $\eta$  all decrease from the respective values which were obtained in the PS case. The lowest value of  $\eta$  turns out to be  $\sim 0.63$ . Notice that a lower value of  $M_C$  is associated with a higher  $M_U$ , which must not exceed  $M_{\text{Planck}}$ .  $M_C$  is also bounded from below by the experimental limits on flavour-changing transitions such as  $K_L \rightarrow \mu e$ . It is this that determines the lowest admissible  $M_C$ , in general. From the inset it is seen that although  $M_U$  increases as  $M_C$  decreases, it remains below  $M_{\text{Planck}}$  so long as  $M_C > 10^6 \text{ GeV}$ . As  $M_C$  increases  $M_D$  increases as well and the point where it meets the decreasing  $M_U$  determines the upper limit of  $M_C$ . For every plot the ranges consistent with  $4 \text{ TeV} \leq M_R \leq 10 \text{ TeV}$  are between the two curves, the solid one indicating the  $M_R = 4 \text{ TeV}$  end. The results are almost insensitive to the choice of  $M_0$  between  $1 \text{ TeV}$  and  $M_R$ . Note that irrespective of the scale of  $SU(4)_C$  breaking,  $M_D$  always remains above  $10^{16} \text{ GeV}$ . The unification coupling constant,  $w_U$ , varies between 38.4 and 47.6 and thus perturbativity remains valid throughout.

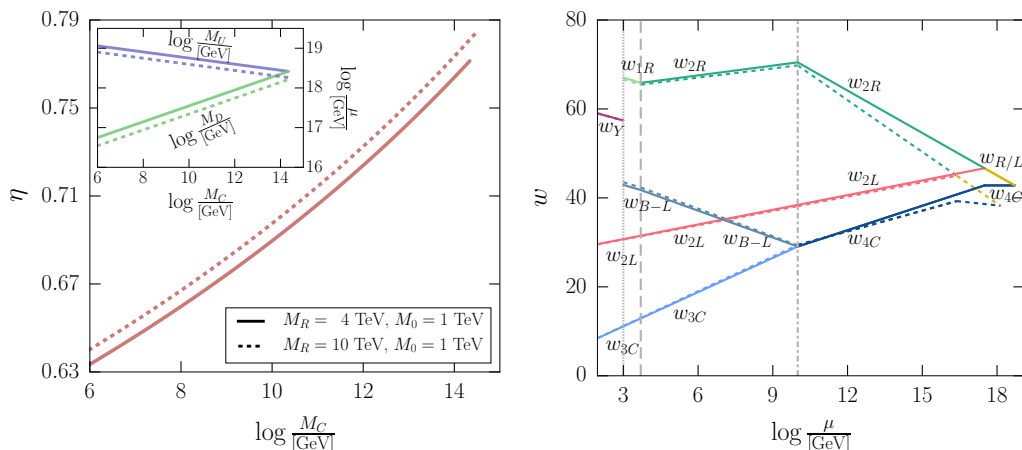


**Figure 5.** Left:  $\eta$  is plotted as a function of  $M_C$  for the DCR chain. In the inset the behaviour of  $M_D$  and  $M_U$  are shown. The two curves in each case correspond to  $M_R = 4$  (solid) and 10 TeV (dashed). In both cases  $M_0 = 1 \text{ TeV}$  is taken. Right: behaviour of the gauge couplings for the DCR chain of SO(10) GUT with  $M_0 = 1 \text{ TeV}$ ,  $M_R = 5 \text{ TeV}$  and  $M_C = 10^{10} \text{ GeV}$ . The solid (dashed) lines correspond to one-loop (two-loop) evolution of couplings. The scalar fields are as in table 3.

The behaviour of the coupling constants as a function of the energy scale for a typical case of  $M_0 = 1 \text{ TeV}$ ,  $M_R = 5 \text{ TeV}$  and  $M_C = 10^{10} \text{ GeV}$  are shown (solid lines) in the right panel of figure 5. Note that due to the contributions of large scalar multiplets to the  $\beta$ -functions the coupling  $g_{2R}$  grows beyond  $M_C$ . Although this chain is suited to our needs, the unification scale is close to the Planck scale for  $M_R \sim \mathcal{O}(\text{TeV})$ . Thus, if  $M_{W_R} \sim \mathcal{O}(\text{TeV})$  then it is unlikely that ongoing proton decay experiments [36] will observe a signal. This is a consequence of our adhering to the principle of minimality of Higgs scalars. One can lower  $M_U$  by including scalars redundant to symmetry breaking.

We have set the lower limit of  $M_C$  at  $10^6 \text{ GeV}$  from the limits on rare meson decays such as  $K_L \rightarrow \mu e$  or  $B_{d,s} \rightarrow \mu e$ . The current limit on the branching ratio for the former process is  $Br(K_L \rightarrow \mu^\pm e^\mp) < 4.7 \times 10^{-12}$  at 90% CL [33] which translates to  $M_C \gtrsim 10^6 \text{ GeV}$ . LHCb has set the tightest bounds on the latter processes. They find (again at 90% CL) [37]  $Br(B_d^0 \rightarrow \mu^\pm e^\mp) < 2.8 \times 10^{-9}$  and  $Br(B_s^0 \rightarrow \mu^\pm e^\mp) < 1.1 \times 10^{-8}$  which yield a weaker limit on  $M_C$ . It can be expected that these bounds will be strengthened when the results from the newer runs of LHC appear. In addition,  $n - \bar{n}$  oscillations can be mediated through coloured scalars belonging to the  $[\bar{10}, 1, 3] \subset \underline{126}$  which also acquire mass at the scale of  $M_C$ . The current experimental limit,  $\tau_{n-\bar{n}} \geq 2.7 \times 10^8 \text{ s}$  [38] at 90% CL, also translates to  $M_C \gtrsim 10^6 \text{ GeV}$ . Therefore, improvements in the measurement of the above-noted rare meson decays and  $n - \bar{n}$  oscillations open the possibility of probing, at least in part, the GUT options that can accommodate a TeV-scale  $W_R$ .

### 6.3 The $M_D = M_U$ case

There are a number of daughter chains of the DCR route with two symmetries breaking at the same scale. Of these, the choice  $M_C = M_R$ , resulting in a common point of the DCR

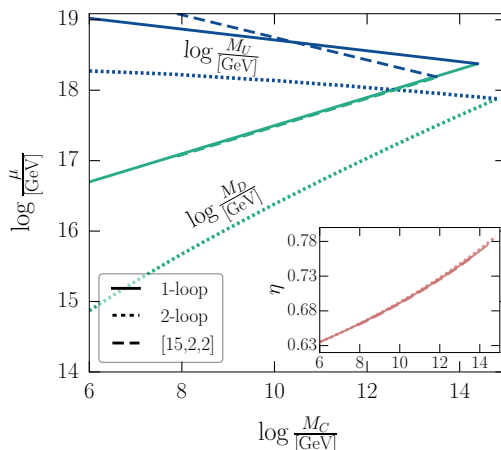


**Figure 6.** A comparison of the results for one-loop (solid lines) and two-loop (dotted line) running. The evolution of  $M_U$  and  $M_D$  with  $M_C$  is displayed. Also shown is the case of one-loop running when a  $[15,2,2]$  scalar multiplet is added (dashed lines). In the inset the variation of  $\eta$  is presented.

and DRC routes, violates the lower bound on  $M_C$  from flavour changing processes since  $M_R \sim \mathcal{O}(\text{TeV})$ . As noted in the previous section, another alternative, namely,  $M_D = M_C$ , which is a point shared by the DCR and CDR routes, occurs at an energy beyond the Planck scale. The only remaining possibility is  $M_D = M_U$ .

The upper limit on  $M_C$  is set by the requirement  $M_D = M_U$ . This happens when D-parity is broken at the GUT scale by a  $[1,1,1]_- \subset \underline{210}$ . We thus have

$$\text{SO}(10) \xrightarrow[\underline{210}]{M_U=M_D} \mathcal{G}_{422} \xrightarrow[\underline{210}]{M_C} \mathcal{G}_{3122} \xrightarrow[\underline{210}]{M_R} \mathcal{G}_{3121} \xrightarrow[\underline{126}]{M_0} \mathcal{G}_{321}. \quad (6.1)$$

From the inset in the left panel of figure 5 it is seen that for  $M_C \sim 2 \times 10^{14}$  GeV one has  $M_D = M_U$ . As this chain has three intermediate steps, there are no free parameters after setting  $M_0$  and  $M_R$ . The coupling at unification,  $w_U$ , comes to be around 47.6, and  $\eta$ , as can be seen from the left panel of figure 5, is near 0.78. An interesting aspect of this chain is that it is minimal in the number of scalar multiplets used.

### 6.4 Two-loop comparison

The discussion till now, based on RG evolution using one-loop  $\beta$ -functions, was amenable to an analytical examination. Our aim was to reason our way through different SO(10) symmetry-breaking options in search of chains which can accommodate a TeV range  $M_R$ . Now, after finding a specific pattern for which  $M_R \sim \mathcal{O}(\text{TeV})$  is tenable, we indicate the size of two-loop effects for this chain. In the right panel of figure 5 the evolution of the couplings for a typical choice of  $M_C = 10^{10}$  GeV,  $M_R = 10$  TeV and  $M_0 = 1$  TeV are indicated by the dashed lines. It is seen that the essential physics is largely unaltered though there is some change in the various energy scales.

The chain in (5.7) contains many scalar fields until  $\text{SU}(4)_C$  breaking, contributing heavily to the two-loop  $\beta$ -coefficients [39–42]. These are responsible for some departures from the one-loop results. We have presented the one-loop results for the DCR route

keeping  $M_C$  as an input parameter. In figure 6 we compare the one-loop (solid lines) and two-loop (dotted lines) results for  $M_U$  and  $M_D$  as a function of  $M_C$ . The deviation for both scales increases with decreasing  $M_C$ . This is intuitive because with lower  $M_C$   $SU(4)_C$  remains a good symmetry for a larger energy range over which the two-loop contributions are effective. In the inset a similar comparison is made for  $\eta$ . It is noteworthy that  $\eta$  remains largely unaffected.

### 6.5 Additional scalars: two examples

If fermion masses are generated through scalars which belong to the minimal set required for symmetry breaking then mass relationships do not reflect observed values. One needs to add at least one extra scalar multiplet — which is light, couples to fermions, and develops a  $vev$  at the electroweak scale — to get realistic mass ratios. In  $SO(10)$ , fermions reside in the  $\underline{16}$  representation and scalars transforming only as  $\underline{120}$ ,  $\underline{126}$ , and  $\underline{10}$  can have Yukawa couplings, since:

$$16 \times 16 = 10 + 120 + 126. \tag{6.2}$$

In  $SO(10)$  GUTs improved fermion mass relations can be obtained [30] using the PS submultiplet  $[15,2,2] \subset \underline{126}$  in addition to the  $[1,2,2] \subset \underline{10}$ . The natural scale for the extra scalar submultiplet would have been at the GUT scale and extra fine-tuning is necessary to keep it at the electroweak scale.

We have examined the behaviour of gauge coupling evolutions for the DCR case including the additional  $[15,2,2]$  submultiplet to check if the TeV range  $M_R$  still remains viable. In figure 6 the variation of  $M_D$  and  $M_U$  with  $M_C$  when an extra  $[15,2,2]$  is included are shown (dashed lines). The effect on  $\eta$  (shown in the inset) is negligible. The important change is that the permitted lowest  $M_C$  is more restricted as  $M_U$  tends rapidly towards  $M_{\text{Planck}}$ .

It is clear that the scale  $M_D$  is governed by the difference in the  $\beta$ -coefficients of  $SU(2)_R$  and  $SU(2)_L$ . Submultiplets such as  $[15,2,2]$ , which contribute symmetrically to the  $\beta$ -coefficients of the left- and right-handed  $SU(2)$  groups, will not affect the difference and so do not change the D-parity breaking scale. For the reasoning  $\eta$  is not affected as well.

Another alternative we examined pertains to the impact of additional scalars necessary to produce two right-handed neutrinos nearly degenerate in mass but with opposite CP-properties. As noted in section 2.1 this can explain the lack of like-sign dilepton events in the CMS data [18]. A right-handed neutrino mass matrix of the appropriate nature can be generated [27] by a scalar multiplet  $\chi \equiv (1,2,1)$  under the  $SU(2)_L \times SU(2)_R \times U(1)_{B-L}$  symmetry. In an  $SO(10)$  GUT  $\chi$  is a member of the  $\underline{16}$  representation and must develop a  $vev$  at the scale  $M_0$ . We have examined the impact of adding a  $\underline{16}$ -plet on  $\eta = g_R/g_L$ , the symmetry breaking scales, and the coupling at the unification point. We find no serious effect on any of these, the allowed range of  $M_C$  is about one order of magnitude larger, and for any  $M_C$ , the unification scale,  $M_U$ , and the D-parity-breaking scale,  $M_D$ , are both somewhat lowered.  $\eta$  is essentially unaffected.

Sr No.	Intermediate Symmetries	Mass Scales $\left(\log \frac{\mu}{[\text{GeV}]}\right)$			$w_U$	$\eta$
		$M_U$	$M_D$	$M_C$		
1	$\mathcal{G}_{422D} \rightarrow \mathcal{G}_{422} \rightarrow \mathcal{G}_{3122} \rightarrow \mathcal{G}_{3121}$	19.02 - 18.38	16.70 - 18.38	6.00 - 14.39	38.41 - 47.63	0.64 - 0.78
2	2-loop	18.27 - 17.88	14.87 - 17.88	6.00 - 14.80	29.54 - 46.66	0.64 - 0.79
3	Added [15,2,2] scalar	$M_{\text{Planck}} - 18.19$	17.06 - 18.19	7.90 - 13.52	18.59 - 37.52	0.66 - 0.76

**Table 4.** The SO(10) symmetry-breaking chains consistent with  $M_R = 5 \text{ TeV}$  and  $M_0 = 1 \text{ TeV}$ . The intermediate symmetries and the associated mass-scales are shown.

## 7 Summary and conclusions

The observation by the CMS collaboration of a  $2.8\sigma$  excess in the  $(2e)(2j)$  channel around 2.1 TeV can be interpreted as a preliminary indication of the production of a right-handed gauge boson  $W_R$ . Within the left-right symmetric model the excess identifies specific values of  $\eta = g_R/g_L$ ,  $r = M_N/M_{W_R}$ , and  $V_{Nee}$ . We stress that even with  $g_R = g_L$  and  $V_{Nee} = 1$  the data can be accommodated by an appropriate choice of  $r$ .

We explore what the CMS result implies if the left-right symmetric model is embedded in an SO(10) GUT.  $\eta \neq 1$  is a consequence of the breaking of left-right D-parity. We find that a  $W_R$  in the few TeV range very tightly restricts the possible routes of descent of the GUT to the standard model. The only sequence of symmetry breaking which is permitted is  $M_D > M_C > M_R > M_0$  with a D-parity breaking scale  $\geq 10^{16} \text{ GeV}$ . All other orderings of symmetry breaking are excluded. Breaking of left-right discrete parity at such a high scale pushes  $g_L$  and  $g_R$  apart and one finds  $0.64 \leq \eta \leq 0.78$ . The unification scale,  $M_U$ , has to be as high as  $\sim 10^{18} \text{ GeV}$  so that it is very unlikely that proton decay will be seen in the ongoing experiments. The SU(4)<sub>C</sub>-breaking scale,  $M_C$ , can be as low as  $10^6 \text{ GeV}$ , which may be probed by rare decays such as  $K_L \rightarrow \mu e$  and  $B_{d,s} \rightarrow \mu e$  or  $n - \bar{n}$  oscillations. In table 4 we summarise the essence of the allowed GUT solutions. We have assumed that no extra scalar multiplets are included beyond those needed for symmetry breaking and invoked the Extended Survival Hypothesis to identify scalar submultiplet masses.

The ATLAS collaboration has indicated [43] an enhancement around 2.1 TeV in the di-boson —  $ZZ$  and  $WZ$  — channels in their 8 TeV data. Our interpretation of the excess in the  $(ee)(jj)$  channel can be extended to include the branching ratio of  $W_R$  to di-boson states [44, 45]. One can arrange to accommodate both these findings if  $r \simeq 1$  and  $V_{Nee} < 1$ . Such a combined analysis is beyond the scope of this work and will be reported elsewhere. Results along somewhat similar directions can be found in the literature [46]. It has also been shown that interpretations of the di-boson observations are possible if the LRS model is embellished with the addition of some extra fermionic states [14, 27].

## Acknowledgments

TB acknowledges a Junior Research Fellowship from UGC, India. AR is partially funded by the Department of Science and Technology Grant No. SR/S2/JCB-14/2009.

**Open Access.** This article is distributed under the terms of the Creative Commons Attribution License ([CC-BY 4.0](https://creativecommons.org/licenses/by/4.0/)), which permits any use, distribution and reproduction in any medium, provided the original author(s) and source are credited.

## References

- [1] J.C. Pati and A. Salam, *Is baryon number conserved?*, *Phys. Rev. Lett.* **31** (1973) 661 [[INSPIRE](#)].
- [2] J.C. Pati and A. Salam, *Lepton number as the fourth color*, *Phys. Rev. D* **10** (1974) 275 [*Erratum ibid.* **D 11** (1975) 703] [[INSPIRE](#)].
- [3] R.N. Mohapatra and J.C. Pati, *Left-right gauge symmetry and an isoconjugate model of CP-violation*, *Phys. Rev. D* **11** (1975) 566 [[INSPIRE](#)].
- [4] R.N. Mohapatra and J.C. Pati, *A natural left-right symmetry*, *Phys. Rev. D* **11** (1975) 2558 [[INSPIRE](#)].
- [5] G. Senjanović and R.N. Mohapatra, *Exact left-right symmetry and spontaneous violation of parity*, *Phys. Rev. D* **12** (1975) 1502 [[INSPIRE](#)].
- [6] H. Georgi, *The state of the art-gauge theories*, *AIP Conf. Proc.* **23** (1975) 575.
- [7] H. Fritzsch and P. Minkowski, *Unified interactions of leptons and hadrons*, *Annals Phys.* **93** (1975) 193 [[INSPIRE](#)].
- [8] CMS collaboration, *Search for heavy neutrinos and W bosons with right-handed couplings in proton-proton collisions at  $\sqrt{s} = 8$  TeV*, *Eur. Phys. J. C* **74** (2014) 3149 [[arXiv:1407.3683](#)] [[INSPIRE](#)].
- [9] CMS collaboration, *Search for heavy neutrinos and  $W_R$  bosons with right-handed couplings in a left-right symmetric model in pp collisions at  $\sqrt{s} = 7$  TeV*, *Phys. Rev. Lett.* **109** (2012) 261802 [[arXiv:1210.2402](#)] [[INSPIRE](#)].
- [10] CMS collaboration, *Search for  $W' \rightarrow tb$  decays in the lepton + jets final state in pp collisions at  $\sqrt{s} = 8$  TeV*, *JHEP* **05** (2014) 108 [[arXiv:1402.2176](#)] [[INSPIRE](#)].
- [11] ATLAS collaboration, *Search for heavy neutrinos and right-handed W bosons in events with two leptons and jets in pp collisions at  $\sqrt{s} = 7$  TeV with the ATLAS detector*, *Eur. Phys. J. C* **72** (2012) 2056 [[arXiv:1203.5420](#)] [[INSPIRE](#)].
- [12] ATLAS collaboration, *Search for tb resonances in proton-proton collisions at  $\sqrt{s} = 7$  TeV with the ATLAS detector*, *Phys. Rev. Lett.* **109** (2012) 081801 [[arXiv:1205.1016](#)] [[INSPIRE](#)].
- [13] J.A. Aguilar-Saavedra and F.R. Joaquim, *Closer look at the possible CMS signal of a new gauge boson*, *Phys. Rev. D* **90** (2014) 115010 [[arXiv:1408.2456](#)] [[INSPIRE](#)].
- [14] B.A. Dobrescu and Z. Liu,  *$W'$  boson near 2 TeV: predictions for Run 2 of the LHC*, *Phys. Rev. Lett.* **115** (2015) 211802 [[arXiv:1506.06736](#)] [[INSPIRE](#)].
- [15] F.F. Deppisch, T.E. Gonzalo, S. Patra, N. Sahu and U. Sarkar, *Signal of right-handed charged gauge bosons at the LHC?*, *Phys. Rev. D* **90** (2014) 053014 [[arXiv:1407.5384](#)] [[INSPIRE](#)].

- [16] F.F. Deppisch, T.E. Gonzalo, S. Patra, N. Sahu and U. Sarkar, *Double beta decay, lepton flavor violation and collider signatures of left-right symmetric models with spontaneous D-parity breaking*, *Phys. Rev. D* **91** (2015) 015018 [[arXiv:1410.6427](#)] [[INSPIRE](#)].
- [17] M. Heikinheimo, M. Raidal and C. Spethmann, *Testing right-handed currents at the LHC*, *Eur. Phys. J. C* **74** (2014) 3107 [[arXiv:1407.6908](#)] [[INSPIRE](#)].
- [18] J. Gluza and T. Jeliński, *Heavy neutrinos and the  $pp \rightarrow lljj$  CMS data*, *Phys. Lett. B* **748** (2015) 125 [[arXiv:1504.05568](#)] [[INSPIRE](#)].
- [19] B.A. Dobrescu and A. Martin, *Interpretations of anomalous LHC events with electrons and jets*, *Phys. Rev. D* **91** (2015) 035019 [[arXiv:1408.1082](#)] [[INSPIRE](#)].
- [20] M.K. Parida and B. Sahoo, *Planck-scale induced left-right gauge theory at LHC and experimental tests*, [arXiv:1411.6748](#) [[INSPIRE](#)].
- [21] D. Chang, R.N. Mohapatra and M.K. Parida, *Decoupling parity and  $SU(2)_R$  breaking scales: a new approach to left-right symmetric models*, *Phys. Rev. Lett.* **52** (1984) 1072 [[INSPIRE](#)].
- [22] D. Chang, R.N. Mohapatra and M.K. Parida, *A new approach to left-right symmetry breaking in unified gauge theories*, *Phys. Rev. D* **30** (1984) 1052 [[INSPIRE](#)].
- [23] D. Chang, R.N. Mohapatra, J. Gipson, R.E. Marshak and M.K. Parida, *Experimental tests of new  $SO(10)$  grand unification*, *Phys. Rev. D* **31** (1985) 1718 [[INSPIRE](#)].
- [24] T.W.B. Kibble, G. Lazarides and Q. Shafi, *Walls bounded by strings*, *Phys. Rev. D* **26** (1982) 435 [[INSPIRE](#)].
- [25] V.A. Kuzmin and M.E. Shaposhnikov, *Baryon asymmetry of the universe versus left-right symmetry*, *Phys. Lett. B* **92** (1980) 115 [[INSPIRE](#)].
- [26] W.-Y. Keung and G. Senjanović, *Majorana neutrinos and the production of the right-handed charged gauge boson*, *Phys. Rev. Lett.* **50** (1983) 1427 [[INSPIRE](#)].
- [27] P.S. Bhupal Dev and R.N. Mohapatra, *Unified explanation of the  $eejj$ , diboson and dijet resonances at the LHC*, *Phys. Rev. Lett.* **115** (2015) 181803 [[arXiv:1508.02277](#)] [[INSPIRE](#)].
- [28] ATLAS collaboration, *Search for heavy Majorana neutrinos with the ATLAS detector in  $pp$  collisions at  $\sqrt{s} = 8$  TeV*, *JHEP* **07** (2015) 162 [[arXiv:1506.06020](#)] [[INSPIRE](#)].
- [29] H. Georgi and C. Jarlskog, *A new lepton-quark mass relation in a unified theory*, *Phys. Lett. B* **86** (1979) 297 [[INSPIRE](#)].
- [30] H. Georgi and D.V. Nanopoulos, *Masses and mixing in unified theories*, *Nucl. Phys. B* **159** (1979) 16 [[INSPIRE](#)].
- [31] F. del Aguila and L.E. Ibáñez, *Higgs bosons in  $SO(10)$  and partial unification*, *Nucl. Phys. B* **177** (1981) 60 [[INSPIRE](#)].
- [32] R.N. Mohapatra and G. Senjanović, *Higgs boson effects in grand unified theories*, *Phys. Rev. D* **27** (1983) 1601 [[INSPIRE](#)].
- [33] PARTICLE DATA GROUP collaboration, K.A. Olive et al., *Review of particle physics*, *Chin. Phys. C* **38** (2014) 090001 [[INSPIRE](#)].
- [34] N.G. Deshpande and R.J. Johnson, *Experimental limit on  $SU(4)_C$  gauge boson mass*, *Phys. Rev. D* **27** (1983) 1193 [[INSPIRE](#)].
- [35] M.K. Parida and B. Purkayastha, *New lower bound on  $SU(4)_C$  gauge boson mass from CERN LEP measurements and  $K_L \rightarrow \mu e$* , *Phys. Rev. D* **53** (1996) 1706 [[INSPIRE](#)].

- [36] SUPER-KAMIOKANDE collaboration, K. Abe et al., *Search for nucleon decay via  $n \rightarrow \bar{\nu}\pi^0$  and  $p \rightarrow \bar{\nu}\pi^+$  in Super-Kamiokande*, *Phys. Rev. Lett.* **113** (2014) 121802 [[arXiv:1305.4391](#)] [[INSPIRE](#)].
- [37] LHCb collaboration, *Search for the lepton-flavor violating decays  $B_s^0 \rightarrow e^\pm\mu^\mp$  and  $B^0 \rightarrow e^\pm\mu^\mp$* , *Phys. Rev. Lett.* **111** (2013) 141801 [[arXiv:1307.4889](#)] [[INSPIRE](#)].
- [38] SUPER-KAMIOKANDE collaboration, K. Abe et al., *The search for  $n-\bar{n}$  oscillation in Super-Kamiokande I*, *Phys. Rev. D* **91** (2015) 072006 [[arXiv:1109.4227](#)] [[INSPIRE](#)].
- [39] D.R.T. Jones, *The two loop  $\beta$ -function for a  $G_1 \times G_2$  gauge theory*, *Phys. Rev. D* **25** (1982) 581 [[INSPIRE](#)].
- [40] M.E. Machacek and M.T. Vaughn, *Two loop renormalization group equations in a general quantum field theory 1. Wave function renormalization*, *Nucl. Phys. B* **222** (1983) 83 [[INSPIRE](#)].
- [41] M.E. Machacek and M.T. Vaughn, *Two loop renormalization group equations in a general quantum field theory 2. Yukawa couplings*, *Nucl. Phys. B* **236** (1984) 221 [[INSPIRE](#)].
- [42] M.E. Machacek and M.T. Vaughn, *Two loop renormalization group equations in a general quantum field theory 3. Scalar quartic couplings*, *Nucl. Phys. B* **249** (1985) 70 [[INSPIRE](#)].
- [43] ATLAS collaboration, *Search for high-mass diboson resonances with boson-tagged jets in proton-proton collisions at  $\sqrt{s} = 8$  TeV with the ATLAS detector*, *JHEP* **12** (2015) 055 [[arXiv:1506.00962](#)] [[INSPIRE](#)].
- [44] J. Brehmer, J. Hewett, J. Kopp, T. Rizzo and J. Tattersall, *Symmetry restored in dibosons at the LHC?*, *JHEP* **10** (2015) 182 [[arXiv:1507.00013](#)] [[INSPIRE](#)].
- [45] K. Cheung, W.-Y. Keung, P.-Y. Tseng and T.-C. Yuan, *Interpretations of the ATLAS diboson anomaly*, *Phys. Lett. B* **751** (2015) 188 [[arXiv:1506.06064](#)] [[INSPIRE](#)].
- [46] F.F. Deppisch et al., *Reconciling the 2 TeV excesses at the LHC in a linear seesaw left-right model*, *Phys. Rev. D* **93** (2016) 013011 [[arXiv:1508.05940](#)] [[INSPIRE](#)].